


Morphology-controlled stabilised polyaniline nanoparticles and their electrorheological properties

Polymers and Polymer Composites
Volume 31: 1–12
© The Author(s) 2023
Article reuse guidelines:
sagepub.com/journals-permissions
DOI: 10.1177/09673911231162800
journals.sagepub.com/home/ppc


CP Allais^{1,2}, PJS Foot¹  and RJ Singer¹

Abstract

Nanoparticles and sub-microparticles of the conducting polymers polyaniline (PANI), polyanisidine (PoANIS) and their copolymers were synthesised, deprotonated and dispersed in viscous media in order to study the influence of their synthetic conditions and of steric stabilisers (cellulose-based materials) on the physical, chemical and morphological characteristics of the polymers. Electrorheological (ER) measurements were performed and related to the polymer properties. The polymer particles had various loadings of stabilisers, depending on the polymer/stabiliser interactions and the stabiliser concentration. When stabilised with hydroxyethylcellulose (HEC), the PANI particles contained traces of HEC, while PoANIS, less stabilised by the electron-rich HEC molecules, did not. Stabilised PANI-HEC synthesised at 0°C readily formed small fibres that, when deprotonated, displayed a large electrorheological response (yield stress ca. 800 Pa at 3.2 kV.mm⁻¹). PoANIS prepared under the same conditions yielded a polydisperse cenospheric material with no ER activity.

Keywords

Electrorheological, stabilised suspensions, polyaniline colloids, hydroxyethyl cellulose, fluids, nanoparticles

Received 30 December 2022; accepted 22 February 2023

Introduction

Organic conducting polymers have developed from scientific curiosities in 1977 to already being important commercial materials nowadays.^{1,2} One of their potential applications with strong current research interest is the development of electrorheological (ER) materials based on conducting polymers in the form of nanoparticles suspended in slightly viscous media such as silicone oil.^{3,4} Their highly anisotropic electrical polarizability is particularly conducive to good ER properties.

Heterocyclic polymers such as polythiophene,⁵ polypyrrole^{5,6} and polyindole⁷ have been investigated for their ER properties. However, polyaniline (PANI) is one of the most studied conducting polymers, due to its particularly good stability and multiple oxidation states. Some notable ER studies on PANI and its derivatives include coatings of the polymers on nanoparticles of carbon,⁸ TiO₂,⁹ clays,¹⁰ zeolites,¹¹ magnetic oxides¹² and graphene oxide,¹³ as well as surfactant-stabilised polymer nanostructures.¹⁴ This field has recently been well reviewed.^{15,16}

The use of polysaccharide derivatives such as celluloses or chitosan as steric stabilisers to produce nanoparticles of polyanilines has long been of interest.^{17–19} Its relative simplicity is an attractive feature, and it offers good scope for morphological control which may be valuable for the production of electrorheological fluids. In the present work, we report studies on the synthesis, morphology and conductivities of a range of stabilised nanoparticles of polyaniline and poly(o-anisidine) polyanisidine (PoANIS), and correlate these properties with the ER performance of the particles when dispersed in silicone oil.

¹School of Life Science, Pharmacy and Chemistry, Kingston University London, Kingston upon Thames, Surrey, UK

²Shell France, Puteaux, France

Corresponding author:

PJS Foot, School of LSPC, Kingston University London, HSSCE Faculty, Penrhyn Road, Kingston upon Thames KT1 2EE, UK.

Email: p.j.foot@kingston.ac.uk



Creative Commons Non Commercial CC BY-NC: This article is distributed under the terms of the Creative Commons Attribution-NonCommercial 4.0 License (<https://creativecommons.org/licenses/by-nc/4.0/>) which permits non-commercial use, reproduction and distribution of the work without further permission provided the original work is attributed as specified on the SAGE and Open Access pages (<https://us.sagepub.com/en-us/nam/open-access-at-sage>).

Experimental

Synthesis of polyaniline samples

PANI stabilised by hydroxyethylcellulose (HEC), deprotonated at different pHs. PANI-HEC was synthesised on a laboratory scale and the product was deprotonated at different pHs to study the influence of the latter on conductivity of the prepared compound (Table 1).

Aniline (Sigma Aldrich) was distilled under vacuum and dissolved (100 g, 1.08 mole) in 1 L HCl (1.08 m) containing HEC (30 g, 3% w/v). The viscous solution was kept stirred in ice (0–5°C) for 1 h before a pre-chilled ammonium persulfate (APS) solution (168 g, 0.74 moles in 500 mL water) was slowly added (1.5 h), after which the final weight per volume percentage of HEC in the solution was 2%. The reaction was stirred while surrounded by ice for a further 10 h.

Subsequent deprotonation was achieved by the addition of aqueous sodium hydroxide and constantly followed using a pH meter. When a stable pH had been achieved, portions of the mixture were taken out, aggregated with an equal volume of ethanol and exhaustively washed with water and acetone prior to drying.

Deprotonated PANIs stabilised by HEC. In view of the future electro-rheological testing of the compounds, a set of experiments (Table 2) was done to produce fully-deprotonated PANI-HEC materials. The syntheses were done on a 10 g monomer scale. Aniline and anisidine were the monomers and the reactions were performed over a 4 h period and left overnight at 4°C prior to deprotonation of the products.

Characterisation of the products

Infrared (IR) spectroscopy. The infrared spectra of the products were recorded using a Perkin Elmer Spectrum One infrared spectrophotometer coupled with a Universal ATR (Attenuated Total Reflectance) Sampling Accessory (crystal: Diamond/ZnSe) which allowed easy recording of the traces for the dark polymer powders.

Thermogravimetric analysis (TGA). Polymer powders were placed on a platinum crucible on a Mettler M3 balance. A Mettler TC 10A low thermal resistance furnace was used to heat the samples at 10 and 20°C/min from 50 to 650°C under air atmosphere. The oven temperature was monitored by a thermocouple located very close to the sample boat. The raw data were processed using the Mettler graphware TA72PS2 software package, exported from Qnix to MS-DOS, and re-plotted using Excel.

Electrical conductivity measurements. Sample conductivities were determined using the van der Pauw four-probe method. Discs (13 mm Ø) of compressed dry powders were prepared using standard 13 mm dies (90 kg.mm⁻² pressure, under vacuum). Their thicknesses were measured accurately using a digital calliper (average of six readings). The set-up comprised a Keithley 617 programmable electrometer and a Keithley 224 current source under computer control.

Scanning electron microscopy. The products were placed on aluminium stubs, using double-sided adhesive tape, and gold-coated using a Polaron E5175 gold sputter coater and an Edwards double-stage high vacuum pump. All particle size analyses were performed on a JEOL-6310 scanning electron microscope (SEM), operated at 15 kV accelerating voltage, controlled by the ISIS 200 software.

Table 1. Preparation of PANI stabilised by HEC, deprotonated at various pHs.

Sample ID	Compound name	Synthetic route	Yield
B2000-0078	PANI-HEC (3%wt) 0°C deprotonated NaOH (pH2.4) then aggregated	Mon:Ox:HCl = 1:0.7:1.5	Overall mass: 71 g Approx. Yield: 61%
B2000-0079	PANI-HEC (3%wt) 0°C deprotonated NaOH (pH3.4) then aggregated	Mon:Ox:HCl = 1:0.7:1.5	
B2000-0080	PANI-HEC (3%wt) 0°C deprotonated NaOH (pH4.4) then aggregated	Mon:Ox:HCl = 1:0.7:1.5	
B2000-0081	PANI-HEC (3%wt) 0°C deprotonated NaOH (pH5.4) then aggregated	Mon:Ox:HCl = 1:0.7:1.5	
B2000-0082	PANI-HEC (3%wt) 0°C deprotonated NaOH (pH6.4) then aggregated	Mon:Ox:HCl = 1:0.7:1.5	
B2000-0083	PANI-HEC (3%wt) 0°C deprotonated NaOH (pH7.4) then aggregated	Mon:Ox:HCl = 1:0.7:1.5	
B2000-0084	PANI-HEC (3%wt) 0°C deprotonated NaOH (pH8.4) then aggregated	Mon:Ox:HCl = 1:0.7:1.5	
B2000-0085	PANI-HEC (3%wt) 0°C deprotonated NaOH (pH9.4) then aggregated	Mon:Ox:HCl = 1:0.7:1.5	
B2000-0086	PANI-HEC (3%wt) 0°C deprotonated NaOH (pH10.4) then aggregated	Mon:Ox:HCl = 1:0.7:1.5	

Table 2. Preparation of fully-deprotonated PANI-HEC materials.

Sample ID	Compound name	Synthetic route	Yield
B2000-0125	PoANIS-HEC 0°C. water, deprotonated NaOH (pH 10.1)	Mon:Ox:HCl = 1:0.5:1 HEC 2% w/v	5.3 g–35%
B2000-0126	PANI-HEC 0°C water, deprotonated NaOH (pH 10.08)	Mon:Ox:HCl = 1:0.5:1 HEC 2% w/v	4.5 g–38%
B2000-0123	PANI-HEC 40°C. water, deprotonated NaOH (pH 10.15)	Mon:Ox:HCl = 1:0.5:1 HEC 2% w/v	3.4 g–29%

X-ray diffractometry (XRD). X-ray diffraction studies of PANI powders were performed on a Bruker-AXS D8 Advance diffractometer (Scan speed $0.02 \text{ degree.s}^{-1}$). The XRD patterns were obtained with $\text{CuK}\alpha$ radiation (0.154 nm), with the Cu anode run at 40 kV and 30 mA , and using a nickel filter. The system was controlled via Bruker XRD Commander software, and the diffractograms were exported to Excel spreadsheets and processed.

Electrorheological testing. 10 and 15 wt.% suspensions of ground (pestle and mortar) powders in dry silicone oil (polydimethylsiloxane, Sigma-Aldrich) were prepared and tested using a computer-controlled Bohlin Visco88 viscometer operating in the geometry of two concentric cylinders using a Searle-type sensor system (with rotor shear rates ranging from 14 to 1100 s^{-1}) and connected to a high-voltage dc power supply (from 0 to 3.2 kV.mm^{-1}). The raw data were exported from Qnix to Excel for analysis.

Results and discussion

Infrared spectroscopy

The IR spectrum of HEC showed vibrations due to the hydroxyl group such as O-H stretching at 3384 cm^{-1} , O-H in-plane deformation at 1352 cm^{-1} , and C-O stretching at 1033 cm^{-1} . Bands centred at 2874 cm^{-1} were assigned to C-H stretching of the alkyl groups, and the C-H deformations and skeletal vibrations blended respectively with the 1352 cm^{-1} and 1153 cm^{-1} vibrations. The latter also included the C-O stretching vibration of the ether groups present. A medium-sized peak was seen at 1638 cm^{-1} for adsorbed water.

IR spectra were recorded of PANI HEC samples prepared using the same stabiliser concentration (2 wt.% of the final reaction volume after addition of the oxidant). Compounds B2000-0126 and B2000-0125 were prepared at 0°C using respectively aniline and *o*-anisidine monomers, whereas B2000-0123 was synthesised at 40°C . All these samples were deprotonated at a final pH of 10.1.

At first, peaks relevant to the stabiliser were not noticed in the spectra of the PANIs which featured the quinoid (1587 cm^{-1}) and benzoid (1492 cm^{-1}) PANI ring vibrations, C-N stretching at 1300 cm^{-1} , polaron bands at ca. 1140 cm^{-1} and C-H out-of-plane vibrations of 828 cm^{-1} . For PoANIS, the first four vibrations were blue-shifted due to the electron-releasing nature of the methoxy group. On closer inspection, some bands were seen that related to stabiliser within the core of the particulate material (at ca. 3300 and 2870 cm^{-1} for hydroxyl and alkyl groups, respectively). These peaks were more pronounced for B2000-0125, partly due to the C-H stretching of the methoxy group (2870 cm^{-1}). A peak at 3300 cm^{-1} is associated with N-H stretching vibrations.

For peaks centred at 1050 cm^{-1} , exactly the same pattern was seen in the PANIs and in HEC, with a broad, strong peak at 1053 cm^{-1} and a sharp shoulder at ca. 1033 cm^{-1} . This was not seen in B2000-0125, suggesting that the interactions between PoANIS and the stabiliser were weaker than those for PANI. A possible explanation of this phenomenon is the higher electron density of PoANIS than that of PANI, so that the stability provided by the electron-rich HEC was weaker for PoANIS than for PANIs. Further observations support this idea, such as the fact that upon dedoping PANI-HEC (compounds B2000-0078 to -0086), the 1050 cm^{-1} -centred peaks became weaker, sharper and more separated, suggesting that dedoping caused partial loss of the stabiliser.

Thermogravimetric analysis

The thermal stabilities of five stabilised PANI samples and three stabilisers were assessed by TGA, and the results are summarised in Table 3.

The thermograms of polymer nanoparticles prepared in the presence of these stabilisers and two others (polyvinyl alcohol (PVA) and polyacrylic acid (PAA)), are presented in Figure 1.

Table 3. Thermogravimetric mass-loss transitions for the stabilisers and stabilised PANIs. (Temperatures are in $^\circ\text{C}$. Note that all thermograms are for as-synthesised polymers, except that of B2000-0140 which was deprotonated to a pH of eight in the reaction medium).

Sample	Peak 1	%	Peak 2	%	Peak 3	%	Peak 4	%	Peak 5	%	% At 543
MC	30–200	3.5			335	85.9			365–643	10.3	100
HEC	30–155	4.3	275	41.7	312	25.5			395–643	16.0	77.0
Chitosan	50–215	10.4	288	46.4					405–643	39.1	96.3
B2000-0029	30–150	2.6	190	7.1					220–643	86.0	73.0
B2000-0031	30–140	5.7	140–225	2.5	270	5.0			285–643	87.0	94.0
B2000-0034	30–140	6.9	223	16.6	325	9.3	363	7.9	380–643	59.8	85
B2000-0040	30–140	7.8	220	8.5					250–643	83.6	80.0
B2000-0140	50–140	5.2	140–360	12.1			380	13.1	418	15.3	
	445	13.1	466	12.8	493					29.0	99.0

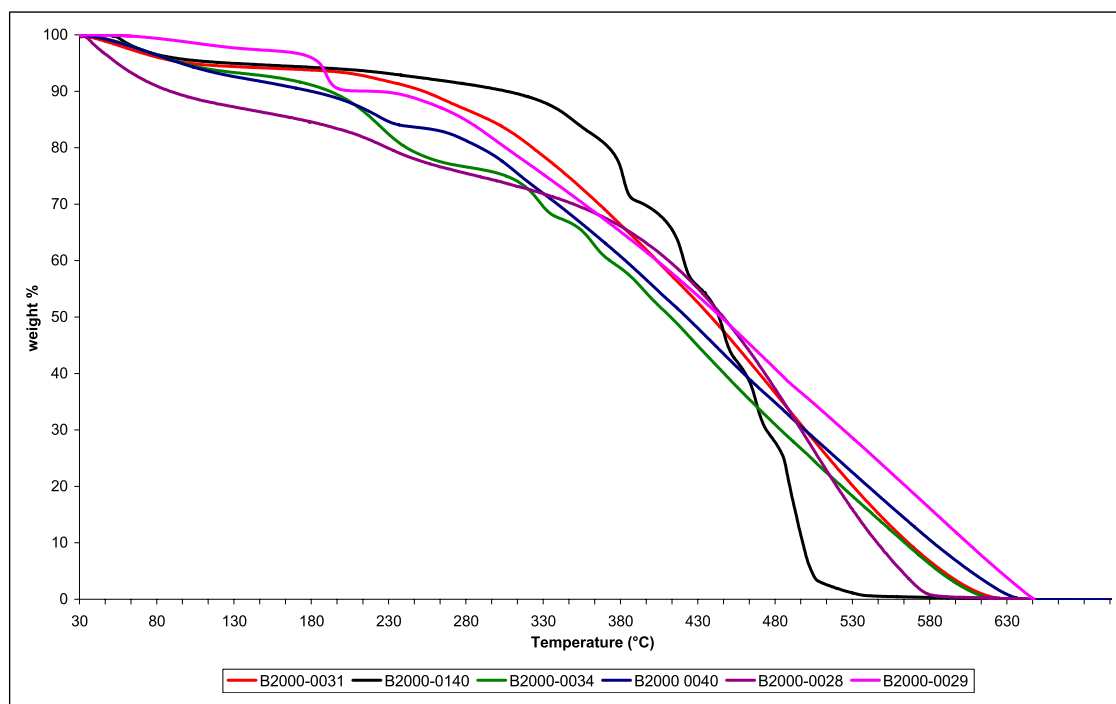


Figure 1. Thermogravimetric (TG) plots of PANIs prepared in stabilised reaction mixtures. (Note that all thermograms are for as-synthesised polymers, except for B2000-0140 which was deprotonated at a stable pH value of eight in the reaction medium).

Figure 1 illustrates three types of thermograms: B2000-0028 (PANI-PAA) has a larger weight loss at low temperatures than the other compounds and a lower temperature of total degradation, while B2000-0140 (PANI-Chitosan) displays better heat resistance than the other compounds up to $\sim 330^{\circ}\text{C}$ but then degrades more quickly in a series of well-defined steps. All the other compounds, i.e. B2000-0029 (PANI-PVA), B2000-0034 (PANI-MC), and B2000-0031/40 (PANI-HEC 0/40 $^{\circ}\text{C}$ respectively), have similar thermal degradation patterns in the backbone decomposition zone and dopant/stabiliser degradation arising at different temperatures.

The noticeable mass-loss at low temperatures for B2000-0028 is probably due to water from the very hydrophilic polyacrylic acid, present either as dopant polyanions or as blended chains within the polymer. Another step is seen at 230°C , due to the loss of HCl from the backbone of the polymer. Backbone degradation is linear and ends at a relatively low temperature, probably due to short chain formation explained by the competition between anilinium radical cations sterically hindered by chains of polyacrylic anions and free radical cations in the reaction mixture.

The absence of any significant amount of protonated imines in B2000-0140 explains its better stability until 330°C because no dopant anion is to be lost. The subsequent steep stair-like decomposition steps are rather unexpected. While the transition seen between 140 and 360°C can be related to the loss observed at 285°C for pure chitosan, the other steps between 380 and 493°C are not in accordance with the usual backbone decomposition of PANI. The low temperature at which all the polymer is degraded suggests the presence of low molecular weight product.

Two possible explanations are proposed. Firstly, chitosan has the same core structure as cellulose, but it possesses pendant amino groups instead of hydroxyl ones. The pKa of chitosan is about 6.2 which is higher than that of aniline. Hence, when dissolving chitosan in dilute HCl prior to the synthesis, some HCl is used up before aniline is poured into the solution, so the pH of the reaction medium is higher than that of conventionally prepared PANI and the polymerisation less favoured. Secondly, when the oxidant is added, some of the ammonium salts of the chitosan could get oxidised as well as the anilinium cations, yielding a copolymer. When a chitosan ammonium radical cation reacts with a growing chain, it quenches the chain growth, yielding low molecular mass polymers. The observed steps could hence be associated with copolymers of different molecular masses.

The four remaining polymers display more conventional thermal degradation. Loss of dopant occurs at 190°C for B2000-0029, and around 220°C for the three methyl and hydroxyethyl cellulose stabilised polymers which could be explained by the presence of stabiliser in the compounds, hindering the paths for the dopant removal. Note that the proportion of dopant is apparently less for B2000-0031 prepared at 40°C , suggesting that at this temperature, the intrinsically doped polymer hydrochloride is partially deprotonated at the end of the synthesis. The volatile HCl molecules in the solution would evaporate out of the reaction medium more quickly at 40°C than at 0°C . The smaller acid concentration would lead the polymer to exchange protons with the solution and hence deprotonate.

Some step-like decomposition features are seen for B2000-0034, with two peaks at 325 and 363°C , which are tentatively attributed to the loss of a separate phase of MC inside the compound.

Morphological characterisation

Derivatives of natural cellulosic compounds such as MC¹⁷ and hydroxypropylcellulose¹⁸ have previously been used to produce stable dispersions of PANI yielding compounds with globular, coral-like and fibrillar morphologies.

In the present work, some compounds of this type were studied by SEM under high and low magnification (Figure 2). Chitosan itself is seen to have a macroscopic flat fibrillar morphology. When used to stabilise PANI products, it is believed to form a covalently-bound chitalin complex¹⁹ resulting from the oxidation of some free primary amine sites on the chitosan anchoring the polymer chains. B2000-0140 consists of a network of fine cylindrical particles ($\Phi \approx 80$ nm) arranged in a “raspberry” morphology.

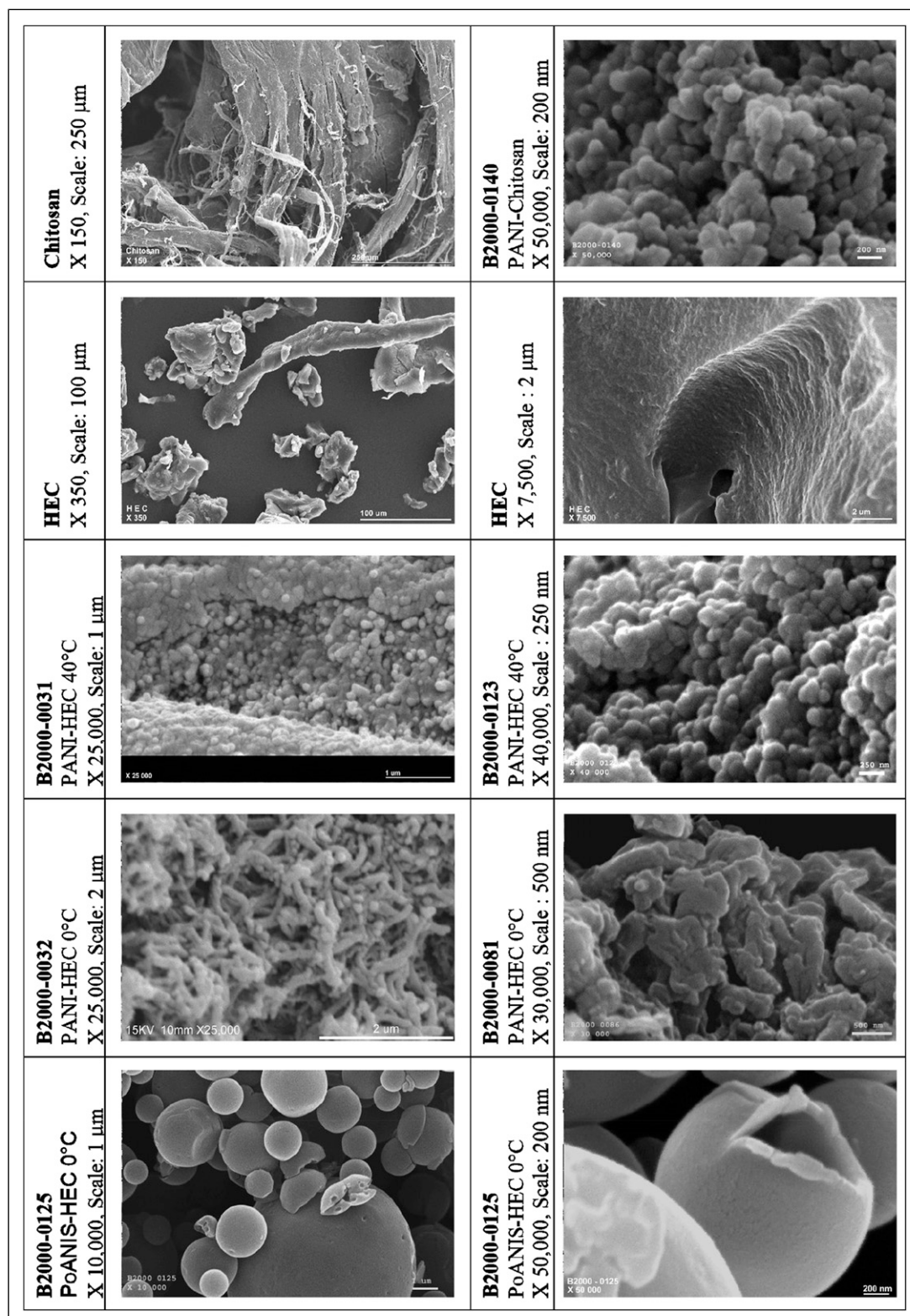


Figure 2. SEM photographs of PANI-cellulosic compounds.

Aldissi et al.²⁰ considered that, in aqueous solution (i.e., a poor solvent), the mixing of two polymeric species such as PANI and PVA leads to steric stabilisation, since the polymers would have more affinity for each other than for the solvent. Figure 3 gives a representation of such a colloidal particle. For our colloids, we suppose that the cellulose outer shell of the micelles has its hydroxyl groups directed towards the aqueous medium and, due to the relatively small amount used (0.85 wt.%), it is thin compared to the internal diameter of the colloid corresponding to the PANI itself.

For PANI-HEC, different morphologies were observed, according to the method and monomers used. The morphology of the stabiliser is that of an amorphous polymer with no obvious macroscopic or microscopic organisation. When PANI-HEC was synthesised at 40°C, the morphologies of as-prepared and dedoped samples were cylindrical ($\Phi \approx 80$ nm), while the compounds prepared at 0°C had the appearance of entangled fibrillar networks of comparable diameter to those of the cylindrical particles prepared at 40°C. Supported by previous work,¹⁸ we believe these fibres result from an ordered stacking of the latter.

At low temperature, the solvent attraction of the grown polymer colloids will be small and adsorption of the stabiliser outer shells will be favoured over inter-particle repulsion.²⁰ The “head to tail” configuration results probably from the charged nature of the polymer entrapped in the stabiliser. Hence there is strong dipole-dipole attraction between the molecules, and the most stable arrangement is that of a fibre where all the particles have their partial positive and negative charges as far apart as possible. When the compound is deprotonated within the reaction medium, these charges become less pronounced and the aggregation is more disparate. When aniline is replaced by anisidine, the effect on morphology is drastic, with a polydisperse cylindrical arrangement ($1 < \Phi < 20$ μm) where many of the particles are cenospheric.

The infrared data (*Infrared Spectroscopy*) indicated that interaction between PoANIS and HEC is weak, since no evidence of HEC vibrations was seen in the spectrum of PoANIS-HEC. We suggest that the presence of HEC inside and outside of the micelles during synthesis pushes the polymeric particles to aggregate towards the colloid's outer walls.

XRD traces of the various deprotonated samples prepared are shown in Figure 4, and the peaks are listed in Table 4. The positions and widths of these peaks were used to calculate the interplanar spacing (d) and crystalline domain width (L) (equivalent to the diameter for spherical particles) using the Bragg and Scherrer equations respectively:

$$d = \lambda / 2 \cdot \sin \theta \quad \text{Bragg equation}$$

$$L = 0.9 \lambda / \Delta(2\theta) \cdot \cos \theta \quad \text{Scherrer equation}$$

where: λ : wavelength of the X-ray source (1.542 Å)

θ : Bragg angle

$\Delta(2\theta)$: FWHM (full width at half maximum height of a given peak)

Previous studies have shown that PANI emeraldine base (EB; formed by deprotonating PANI-HCl) is an almost amorphous compound while PANI-HCl displays some crystallinity.²¹⁻²³ It has also been shown that after dissolution of EB and film casting/stretching, more ordered structures could be obtained. In the present work, one can distinguish three types of XRD patterns. Firstly, for PANI-HEC prepared at 40°C and PANI-Chitosan (cylindrical particles), only one broad peak is seen, centred at 20° (d spacing ≈ 4.5 Å). (Such broad structures are characteristic of amorphous polymers like pure EB, as observed by Pouget et al.²³) No contribution from HEC is seen that would signal its blended presence in PANI-HEC.

PANI-Chitosan displays two broad peaks centred at ca. 10 and 20°²⁴; the first may possibly result from remaining traces of PANI-HCl in the polymers prepared.²³ There is no clear indication that the final particles, after washing, still contain stabiliser.

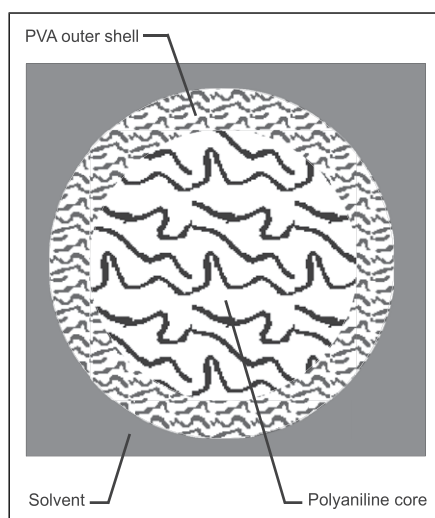


Figure 3. Representation of a PVA-stabilised PANI colloid particle.

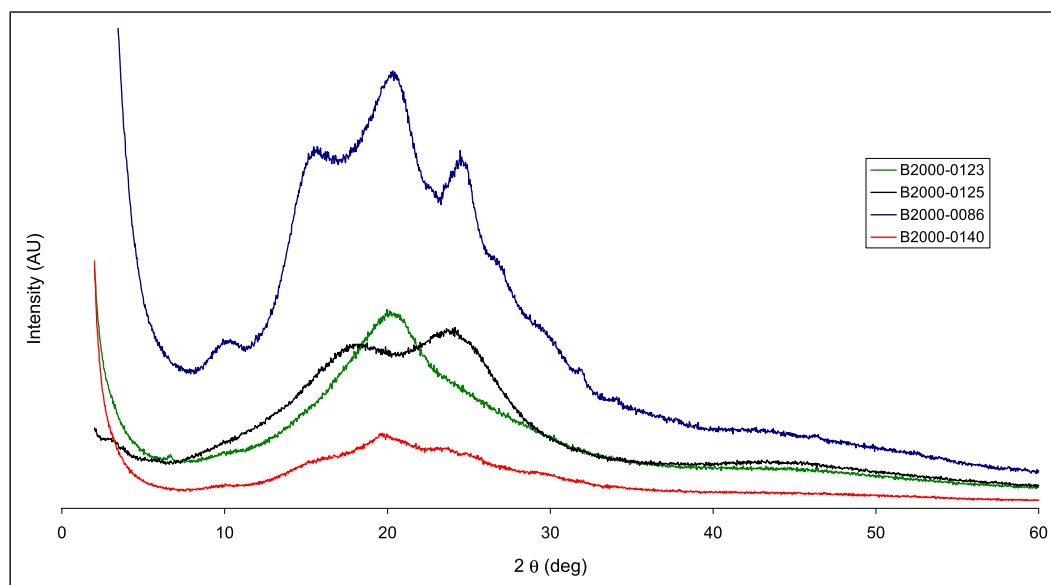


Figure 4. XRD patterns for stabilised PANI and PoANIS composite materials.

Table 4. XRD calculations for PANI and PoANIS nanoparticles.

	$2\theta^\circ$	$\Delta 2\theta^\circ$	L (Å)	d (Å)
B2000-0086	10.22	5.11	45	8.66
	15.80	7.90	26	5.61
	20.42	10.21	20	4.35
	24.62	12.31	27	3.62
B2000-0123	20.39	10.20	15	4.36
B2000-0125	17.99	9.00	10	4.93
	23.90	11.95	13	3.72
B2000-0140	19.70	9.85	16	4.51

For PANI-HEC prepared at 0°C , four peaks rise above the amorphous contribution, as a result of the ordered fibrillar nature of the compound. The domain length of the 10.2° peak corresponds to primary PANI particle size, i.e., 4.5 nm, in accordance with that in pure PANI-HCl.²³ This indicates that PANI would only get associated with the stabiliser after primary aggregation, i.e. when the polymeric particle is too large to remain soluble.

For the centrospheric PoANIS-HEC, the main reflection is divided into two large amorphous peaks confirming the vestigial remains of crystallinity after deprotonation. However, low-angle reflections are absent or too weak to rise above the baseline.

Electrorheological testing of dispersed particles

Most PANI derivatives synthesised by oxidative polymerisation using acids such as hydrochloric or sulphuric acid have polydisperse “rock-spherical” morphologies. They form chains when suspended in oil under an applied electric field by virtue of dipolar attractions. We have shown that under suitable conditions, PANI can be obtained as elongated particles, and it was anticipated (Figure 5) that a suspension of such particles would react much more strongly than a suspension of spherical particles to the application of an electric field (i.e. the individual dipole moments would be enhanced by increasing the distance between the positive and negative halves).

It was envisaged that a smaller size of the dispersed particles would enhance the ER sensitivity due to the increase of the overall number of dipoles formed in the suspension upon the application of an electric field (Figure 6). It would also favour the stability of the system, as small particles would aggregate less easily than large ones.

Dispersions of the stabilised PANI particles were prepared and their ER properties measured in the Warsaw University of Technology, Poland, thanks to the kind provision of Prof. Janusz Plochanski and Dr. Ana Godzalik and their expertise in the field.^{25,26} Suspensions of ground (pestle and mortar) powders in dry silicone oil (polydimethylsiloxane, $\sigma \approx 10^{-13} \text{ S cm}^{-1}$) were prepared and tested using a computer-controlled Bohlin Visco88 viscometer operating in the geometry of two concentric cylinders and connected to a high-voltage dc power supply.

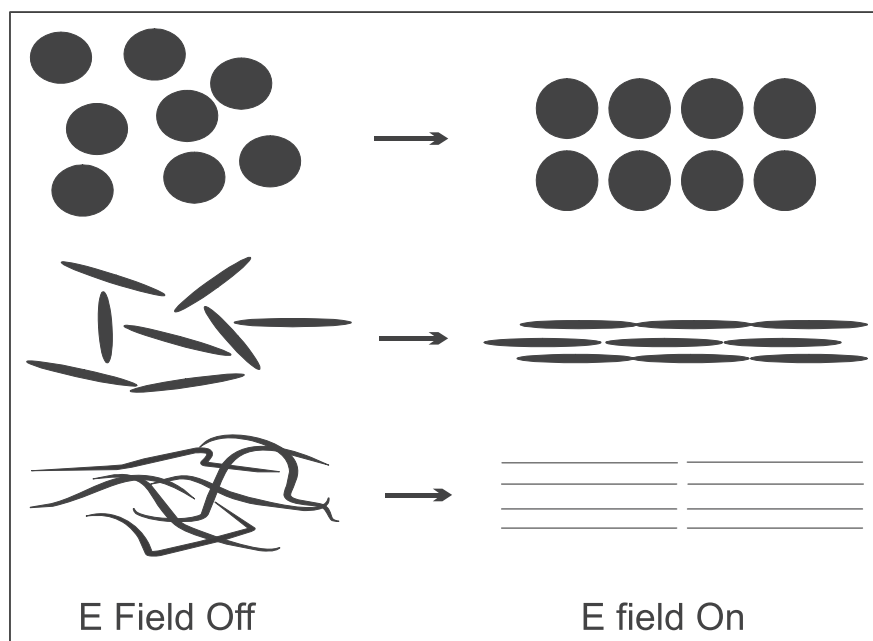


Figure 5. Expected alignments of particles of different shapes under electric field.

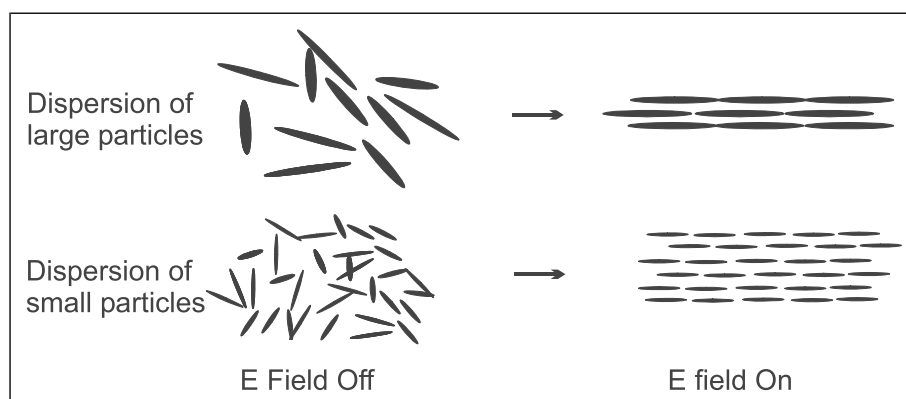


Figure 6. Large and small particles dispersions and electric field effects.

The results are presented in [Figure 7](#). Fibrillar PANI-HEC synthesised at 0°C was studied in suspensions of 15 and 10% (B2000-0086 and B2000-0126 respectively) and both as a “wet” sample (B2000-0086) with no exhaustive vacuum drying to ensure complete removal of water or as a “dry” compound (B2000-0086*).

One can observe a significant decrease in the “static” ER effect when the polymer concentration drops from 15 to 10 wt.%. When a shear force is applied, the effect is even weaker at 10 wt.% due to the impossibility of the suspended particles forming stable chain-like structures.

The ER curves for B2000-0126 under flow reveal that the response to an applied electric field, even at moderate shear rates, approaches that of the suspension at zero field. The calculated relative viscosity at zero electric field also drops dramatically by a factor of ten, so that for low concentrations of suspended particles, the suspension properties approach those of the continuous phase. The difference in ER response between 10 and 15 wt.% suspensions is seen in [Figure 8](#).

For all the suspensions, the shear stress rose monotonically with increasing electric field. A 15-fold decrease in the static yield stress was observed when the suspension concentration fell to 10 wt.%. Similar trends have been reported by other authors.^{26,27} The same behaviour as that of B2000-0126 was found for all the compounds studied as 10 wt.% suspensions.

The polydisperse cenospheric sample B2000-0125 did not display any ER effect (as previously reported²⁷), leading to the conclusion that in this case, the absence of electric field response is related to the intrinsically low polarisability of PoANIS. The presence of ethoxy²⁷ or methoxy groups on the backbone stabilises the electric charge density uniformly in the polymeric particles and therefore, no dipoles are formed upon application of an electric field. A very small ER effect is observed for B2000-0123. We believe the effect is sustained due to the high particle concentration in the suspension of very fine cylindrical particles for PANI-HEC prepared at 40°C. As mentioned earlier, the small size of the particles dispersed will increase the number of dipoles at a given concentration and hence optimise the effect. PANI-Chitosan (B2000-0140) has the same morphological characteristics as B2000-0123 and so again, an ER response is seen. The shapes of the curves are similar to

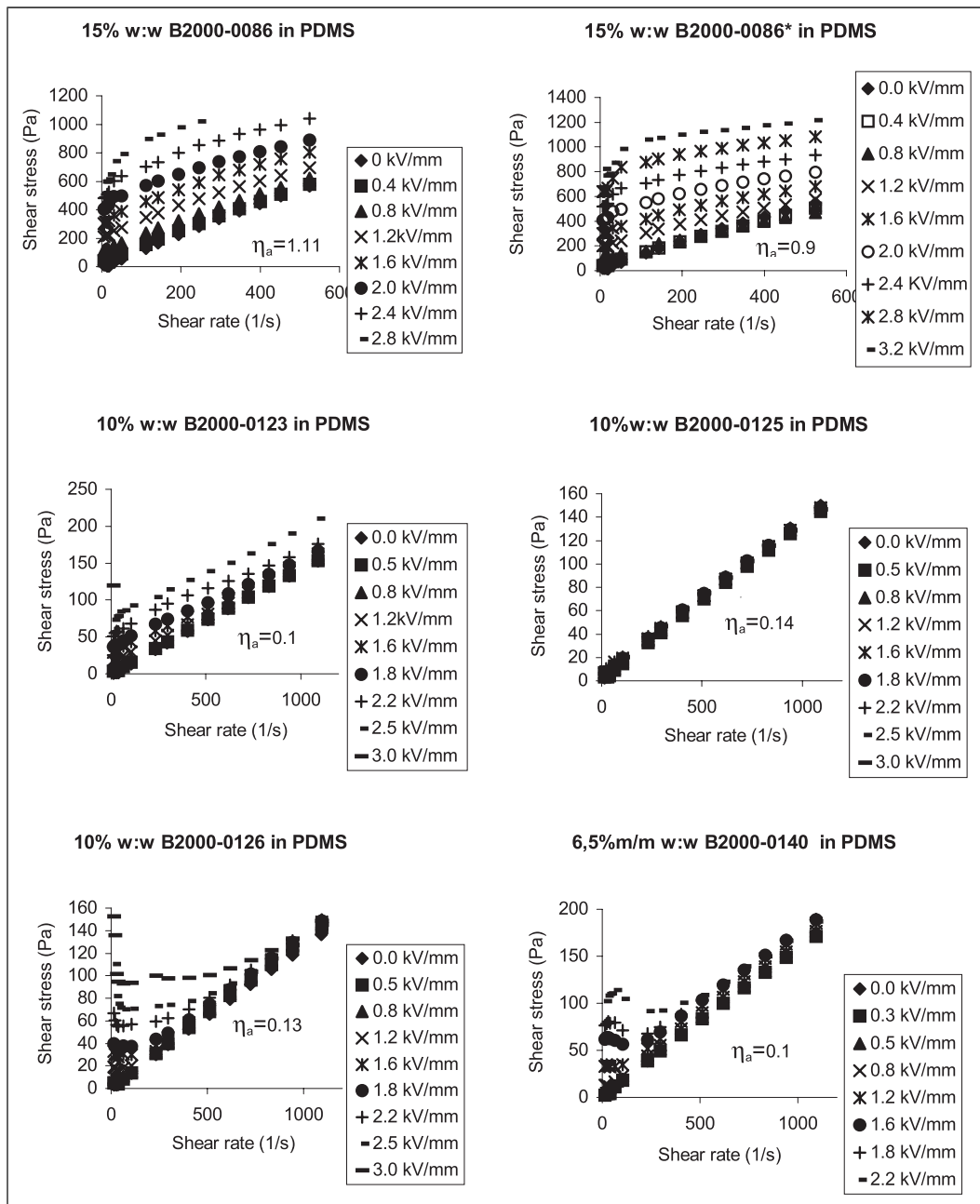


Figure 7. Shear stress versus shear rate for stabilised polyaniline dispersions at different electric field strengths (values for apparent viscosity at 0 kV.mm⁻¹; η_a in Pa.s).

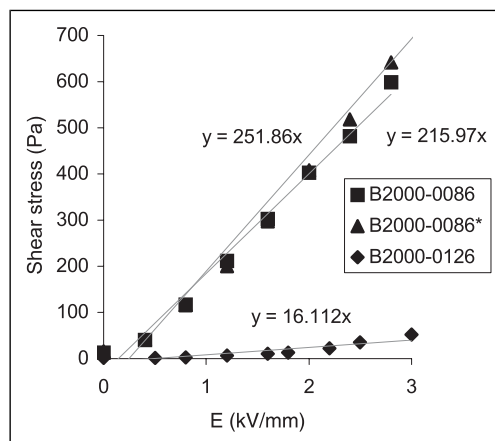


Figure 8. Static shear stress (Pa) versus electric field strength (kV/mm) for cellulose-stabilised PANI suspensions.

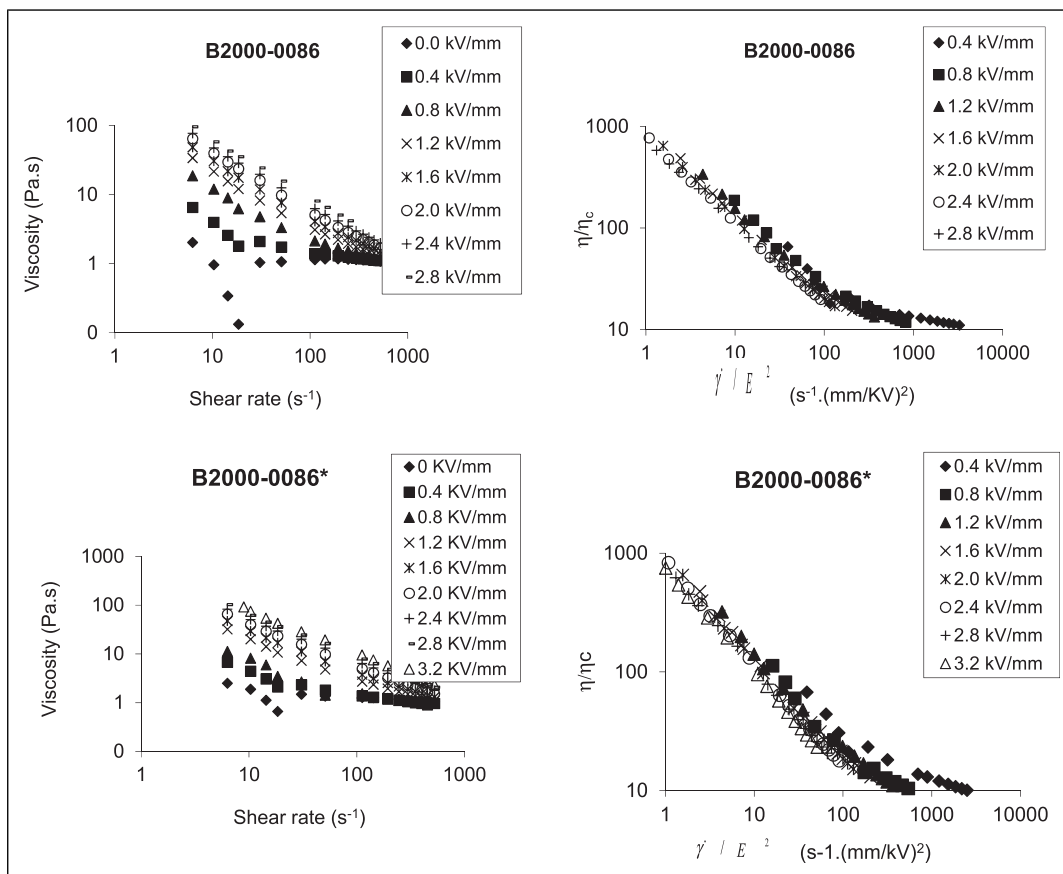


Figure 9. Suspension viscosity, with and without scaling with that of the continuous phase for 15% wt. suspensions of PANI HEC prepa.

Table 5. ER characteristics of PANI materials.

Sample ID	Wt.%	σ (S.cm ⁻¹)	Morphology	η_{a-0} field (Pa.s)	τ_{max} (Pa)
B2000-0086	15	5.5×10^{-10}	Fibres $\approx 100 \times 500$ nm	0.90	599 (2.8 kV.mm ⁻¹)
B2000-0086*	15	—	Fibres $\approx 100 \times 500$ nm	1.11	824 (3.2 kV.mm ⁻¹)
B2000-0123	10	2.2×10^{-9}	Spheres $\varnothing \approx 80$ nm	0.10	120 (3.0 kV.mm ⁻¹)
B2000-0125	10	9.4×10^{-9}	Cenospheres $\varnothing \approx 0.1-10$ μ m	0.14	10 (3.0 kV.mm ⁻¹)
B2000-0126	10	6.0×10^{-10}	Fibres $\approx 100 \times 500$ nm	0.13	152 (3 kV.mm ⁻¹)
B2000-0140	10	4.6×10^{-8}	Spheres $\varnothing \approx 100$ nm	0.16	102 (2.2 kV.mm ⁻¹)

those for B2000-0126, i.e., above a certain shear rate, the suspensions at different electric fields all start behaving like the zero-field one.

Regarding the wet and dry suspensions^{28,29} and the difference in electric field response between B2000-0086 and 0086*: in certain systems, ER effects are strongly affected by the presence of water (considered in these cases as an additive) since it can increase the relative permittivity of the dispersed particles. Another factor²⁸ is linked to the ability of water to form bridges between adjacent particles and hence strengthen their fibrillation capacity. However, in the present study, water (low concentration) did not significantly affect the ER response. Surprisingly, the effect was more a slight degradation of the response than an improvement, and the explanation may be that water would mobilise residual chloride counter-ions in the polymers, causing undesirable ionic conductivity within the suspension; this is supported by the electrical breakdown observed at 3.2 kV.mm⁻¹ in B2000-0086.

The influence of the shear rate on the viscosity of the suspensions was studied, as well as that of the shear rate over the square of the electric field value on the normalised viscosity for the fibrillar B2000-0086 and 0086* (Figure 9). For both compounds, the greatest viscosity increase was observed at low shear rates and high electric field, which is understandable due to the fibrillation of the particles arising only when the shear rate is below a critical value as mentioned before. A sudden drop in viscosity was noted for both samples at zero to low electric field in the region of 20 s⁻¹. For B2000-0086, the minimum value observed is 0.13 Pa s, i.e., almost that of the continuous phase. This phenomenon is strange, since it implies an abrupt cessation of inter-particle interactions at a given shear rate, so the suspension behaves like the continuous phase. When plotted as a function of $\dot{\gamma}/E^2$, the relative viscosities collapse into a single curve, almost linear for the whole $\dot{\gamma}/E^2$ range. Thus it can be seen that the effect is maximised at low shear rate and high electric field.

Conclusion

In this work, colloids of conducting polyanilines were prepared by dispersing the monomers in a solution containing a matrix polymer with which they would interact (before and during the polymerisation). On the basis of the SEM microscopy, IR spectroscopy and XRD analysis data, the polymers were formed as submicro- or nanoparticles.

Table 5 gives an overview of the ER results for PANI particles, along with some of their physical properties collected during the present study.

Based on conducting model predictions, the suspended particles should have a conductivity higher than that of the suspending medium in order to display a positive ER effect. All the dispersed polymer samples had conductivities higher than that of the silicone oil used and they comprehensively displayed positive ER effects. However, electrical breakdown of the suspensions did not occur according to the conductivity of the dispersed particles. For example, the 15 wt.% suspension of B2000-0140 ($4.6 \times 10^{-8} \text{ S cm}^{-1}$) could be analysed with electric field values up to 1.6 kV mm^{-1} while that of the less conductive B2000-0020 suffered electrical breakdown under quite low-field conditions. These observations favour an alternative ER model for PANI materials, based on the relative permittivity (ability of a material to intensify an electric field within itself) or dielectric loss (proportion of the energy lost as heat). The latter model also predicts a greater ER effect with increasing particle concentration, and that it scales with the squared electric field value. Both these predictions were confirmed in our study.

It was also found that the presence of small amounts of adsorbed water in the suspended particles reduced the ER effect, leading us to discard a water-bridge mechanism in our samples. One last factor usually omitted in ER analysis is the influence of the size and shape of the dispersed particles on the ER effect. Although relatively few compounds were tested, it is worthwhile to point out that for the cellulose-stabilised PANI materials, the best ER effects were achieved when the particulates were small and fibrillar (provided that they were re-dispersable). The overall best candidates for ER dispersions of PANI were the small, elongated, HEC-stabilised PANI nanoparticles.

Declaration of conflicting interests

The author(s) declared no potential conflicts of interest with respect to the research, authorship, and/or publication of this article.

Funding

The author(s) disclosed receipt of the following financial support for the research, authorship, and/or publication of this article: The author(s) thank Kingston University London for the award of a Ph.D bursary to CA.

ORCID iD

PJS Foot  <https://orcid.org/0000-0002-2122-3129>

References

1. Trivedi DC. In: Nalwa HS (ed) Conductive polymers: synthesis and electrical properties, *Handbook of organic conductive molecules and polymers*. New York, NY: John Wiley and Sons Inc., 1997; 2.
2. Foot PJS and Kaiser AB. Conducting polymers. *Kirk-Othmer encyclopedia of chemical technology*. New York, NY: John Wiley and Sons Inc., 2004.
3. Lu Q, Han WJ and Choi HJ. Smart and functional conducting polymers: application to electrorheological fluids. *Molecules* 2018; 23(11): 2854. DOI: [10.3390/molecules23112854](https://doi.org/10.3390/molecules23112854).
4. Dong YZ, Kim HM and Choi HJ. Conducting polymer-based electro-responsive smart suspensions. *Chem Pap* 2021; 75(10): 5009–5034. DOI: [10.1007/s11696-021-01550-w](https://doi.org/10.1007/s11696-021-01550-w).
5. Lee S, Noh J, Jekal S, et al. Hollow TiO₂ nanoparticles capped with polarizability-tunable conducting polymers for improved electrorheological activity. *Nanomaterials* 2022; 12(19): 3521. DOI: [10.3390/nano12193521](https://doi.org/10.3390/nano12193521).
6. Yoon CM, Cho KH, Jang Y, et al. Synthesis and electroresponse activity of porous polypyrrole/silica-titania core/shell nanoparticles. *Langmuir* 2018; 34(51): 15773–15782. DOI: [10.1021/acs.langmuir.8b02395](https://doi.org/10.1021/acs.langmuir.8b02395).
7. Esmailnezhad E and Choi HJ. Polyindole nanoparticle-based electrorheological fluid and its green and clean future potential conformance control technique to oil fields. *J. Clean. Prod* 2019; 231: 1218–1225. DOI: [10.1016/j.jclepro.2019.05.341](https://doi.org/10.1016/j.jclepro.2019.05.341).
8. Santos J, Goswami S, Calero N, et al. Electrorheological behaviour of suspensions in silicone oil of doped polyaniline nanostructures containing carbon nanoparticles. *J Intell Mater Syst Struct* 2019; 30(5): 755–763. DOI: [10.1177/1045389X18818776](https://doi.org/10.1177/1045389X18818776).
9. Roosz N, Euvrard M, Lakard B, et al. A straightforward procedure for the synthesis of silica@polyaniline core-shell nanoparticles. *Colloids Surf. A: Physicochem. Eng. Asp* 2019; 573: 237–245. DOI: [10.1016/j.colsurfa.2019.04.036](https://doi.org/10.1016/j.colsurfa.2019.04.036).
10. Zhu YR, Iroh JO, Rajagopalan R, et al. Optimizing the synthesis and thermal properties of conducting polymer-montmorillonite clay nanocomposites. *Energies* 2022; 15(4): 1291. DOI: [10.3390/en15041291](https://doi.org/10.3390/en15041291).
11. Chattopadhyay A, Rani P, Srivastava R, et al. Electro-elastoviscous response of polyaniline functionalized nano-porous zeolite based colloidal dispersions. *J Colloid Interface Sci* 2018; 519: 242–254. DOI: [10.1016/j.jcis.2018.02.066](https://doi.org/10.1016/j.jcis.2018.02.066).
12. Kim HM, Jeong JY, Kang SH, et al. Dual electrorheological and magnetorheological behaviors of poly(N-methyl aniline) coated ZnFe₂O₄ composite particles. *Materials* 2022; 15(7): 2677. DOI: [10.3390/ma15072677](https://doi.org/10.3390/ma15072677).

13. Yuan JH, Wang YD, Xiang LQ, et al. Understanding the enhanced electrorheological effect of reduced graphene oxide-supported polyaniline dielectric nanoplates by a comparative study with graphene oxide as the support core. *IET Nanodielectrics* 2021; 4(3): 143–154. DOI: [10.1049/nde2.12021](https://doi.org/10.1049/nde2.12021).
14. Han WJ and Choi HJ. Synthesis of conducting polymeric nanoparticles in the presence of a polymerizable surfactant and their electrorheological response. *Colloid Polym Sci* 2019; 297(5): 781–784. DOI: [10.1007/s00396-019-04497-3](https://doi.org/10.1007/s00396-019-04497-3).
15. Sebastian J and Samuel JM. Recent advances in the applications of substituted polyanilines and their blends and composites. *Polym Bull (Berl)* 2020; 77(12): 6641–6669. DOI: [10.1007/s00289-019-03081-7](https://doi.org/10.1007/s00289-019-03081-7).
16. Dong YZ, Han WJ and Choi HJ. Polyaniline coated core-shell typed stimuli-responsive microspheres and their electrorheology. *Polymers* 2018; 10(3): 299. DOI [10.3390/polym10030299](https://doi.org/10.3390/polym10030299).
17. Chattopadhyay D and Mandal BM. Methyl cellulose stabilized polyaniline dispersions. *Langmuir* 1996; 12(6): 1585–1588.
18. Stejskal J, Spirkova M, Riede A, et al. Polyaniline dispersions 8. The control of particle morphology. *Polymer* 1999; 40: 2487–2492.
19. Yang S, Tirmizi SA, Burns A, et al. Chitiline materials: soluble chitosan-polyaniline copolymers and their conductive doped forms. *Synth. Met* 1989; 32: 191–200.
20. Aldissi M and Ames SP. Colloidal dispersions of conducting polymers. *Prog. Org. Coat* 1991; 19: 21–58.
21. Joo J, Long SM, Pouget JP, et al. Charge transport of the mesoscopic metallic state in partially crystalline polyanilines. *Phys Rev B* 1998; 57(16): 9567–9580.
22. Lux F. Properties of electronically conductive polyaniline: a comparison between well-known literature data and some recent experimental findings. *Polymer* 1994; 35(14): 2915–2936.
23. Pouget JP, Jozefowicz ME, Epstein AJ, et al. X-ray structure of polyaniline. *Macromolecules* 1991; 24: 779–789.
24. Jaworska M, Sakurai K, Gaudon P, et al. Influence of chitosan characteristics on polymer properties. I: Crystallographic properties. *Polym Int* 2003; 52: 198–205.
25. Gozdalik A, Wycislik H and Plochanski J. Electrorheological effect in suspensions of polyaniline. *Synth. Met* 2000; 109(1–3): 147–150.
26. Plochanski J, Rozanski M and Wycislik H. Electrorheological effect in suspensions of conductive polymers. *Synth. Met* 1999; 102: 1354–1357.
27. Kim JW, Jang W, Choi H, et al. Synthesis and electrorheological characteristics of polyaniline derivatives with different substituents. *Synth. Met* 2001; 119(1–3): 173–174.
28. Parthasarathy M and Klingenberg D. Electrorheology: mechanisms and models. *Mater. Sci. Eng. R Rep* 1996; 17: 57–103.
29. Hao T. Electrorheological suspensions. *Adv Colloid Interface Sci* 2002; 97(1–3): 1–35.